

SCALING RELATIONS FOR TURBULENCE IN MULTIPHASE INTERSTELLAR MEDIUM

ALEXEI G. KRITSUK¹ AND MICHAEL L. NORMAN

Department of Physics and Center for Astrophysics and Space Sciences, University of California at San Diego,
9500 Gilman Drive, La Jolla, CA 92093-0424; akritsuk@cosmos.ucsd.edu, mnorman@cosmos.ucsd.edu

Submitted to *ApJ Letters*, December 30, 2018

ABSTRACT

We simulate the dynamics of phase transition in radiatively cooling interstellar gas in three dimensions with a high order hydrodynamic method. We have previously shown (Kritsuk & Norman 2002a) in simulations with non-equilibrium initial conditions that thermal instability induces supersonic turbulence as a by-product of the phase transition which leads to formation of multiphase medium. We rely on a generalization of the She & L ev eque (1994) model to study velocity scaling relations in this decaying turbulence and compare those with analogous results for compressible isothermal turbulence. Since radiative cooling promotes nonlinear instabilities in highly supersonic flows, turbulence in our simulations tends to be more intermittent than in the isothermal case. Hausdorff dimension of the most singular dissipative structures, D , can be as high as 2.3, while in supersonic isothermal turbulence D is limited by a more primitive nature of dissipation (shocks): $D \leq 2$. We also show that single-phase velocity statistics carry only incomplete information on turbulent cascade in a multiphase medium. We discuss possible implications of these results to hierarchical structure of molecular clouds and star formation.

Subject headings: hydrodynamics — instabilities — ISM: structure — turbulence

1. INTRODUCTION

Interstellar turbulence is believed to be neither incompressible nor isotropic nor homogeneous. Yet the observed velocity scaling relations in quite a variety of environments are surprisingly close to those predicted by Kolmogorov (1941a, K41) theory (Larson 1979, 1981; Armstrong, Rickett, & Spangler 1995). At the same time, turbulence in molecular clouds appears to be quite different in terms of velocity correlations, in some cases, with substantially super-Kolmogorov power indices for both first order velocity structure functions and velocity power spectra (Brunt & Heyer 2002). Interstellar turbulence is one of the key ingredients of modern theories of star formation. It appears to be the major shaping agent for the mass distribution of prestellar dense cores in star forming molecular clouds and, ultimately, it could determine the stellar initial mass function (Padoan & Nordlund 2002). Therefore, it is important to understand what makes it so similar to incompressible Kolmogorov turbulence and when, where, and to what extent one should expect to see significant deviations of observed scaling relations from the predictions of K41 theory.

As is known, dissipation controls scaling properties of turbulence through intermittency. Intermittency corrections to K41 theory for incompressible turbulence, where the most singular dissipative structures are one-dimensional vortex filaments (She & L ev eque 1994, SL94), are different from those for compressible supersonic turbulence, where the structures are two-dimensional shock fronts (Boldyrev 2002, B02). Direct numerical simulations of compressible isothermal turbulence lend support to this heuristic theory, based on the assumption of a log-Poisson energy cascade, demonstrating that dimensionality D of the most extreme dissipative structures depends on the turbulent Mach number and changes from $D = 1$ for subsonic flows to $D = 2$ for highly supersonic flows (Padoan et al. 2003).

Obviously, the nature of dissipative processes in the interstellar medium (ISM) is distinct from that in most laboratory environments as well as in numerical simulations which assume

ideal (magneto)hydrodynamics. What would the most dissipative structures look like in the turbulent ISM where physical conditions are largely determined by competing cooling and heating processes? The shape of the net cooling function is known to be responsible for thermal instability (TI) (Field 1965) which affects the ISM hydrodynamics in a number of ways, from creating multiple thermal phases coexisting at constant pressure (Pikel'ner 1968; Field, Goldsmith, & Habing 1969) to promoting nonlinear instabilities in cold shock bounded slabs (Vishniac 1994; Blondin & Marks 1996). How effective are volumetric energy sources in shaping the velocity scalings in intermittent interstellar turbulence? We address this question here by means of three-dimensional numerical simulations of decaying hydrodynamic turbulence initiated by rapid thermally unstable radiative cooling. In this model turbulence is a by-product of phase transition in the hot gas which leads to the formation of a two-phase medium. This letter is the third in our series on turbulence in multiphase ISM (Kritsuk & Norman 2002a,b). We refer the reader to our previous papers for simulation details which are not covered here.

2. MODEL DESCRIPTION

We start the simulation with a periodic box of 5 pc on a side filled with hot (2×10^6 K) thermally unstable gas initially far from thermal equilibrium (only 2% of radiative cooling is compensated for by a constant uniform volumetric heating source). Small isobaric random Gaussian density perturbations (power spectrum index -3) are imposed to initiate TI while initial velocities are set to zero. We follow the formation of turbulent two-phase medium with the Piecewise Parabolic Method (PPM) of Colella & Woodward (1984) on a grid of 256^3 zones. The equilibrium cooling function we use describes radiative energy losses for solar metallicity gas at temperatures $T \in [10, 10^8]$ K.

With initial gas density of 1 cm^{-3} the timescales for cooling and TI are of the order of ~ 0.1 Myr. The evolution begins with isobaric linear growth of the density perturbations

¹ Also Sobolev Astronomical Institute, St. Petersburg State University

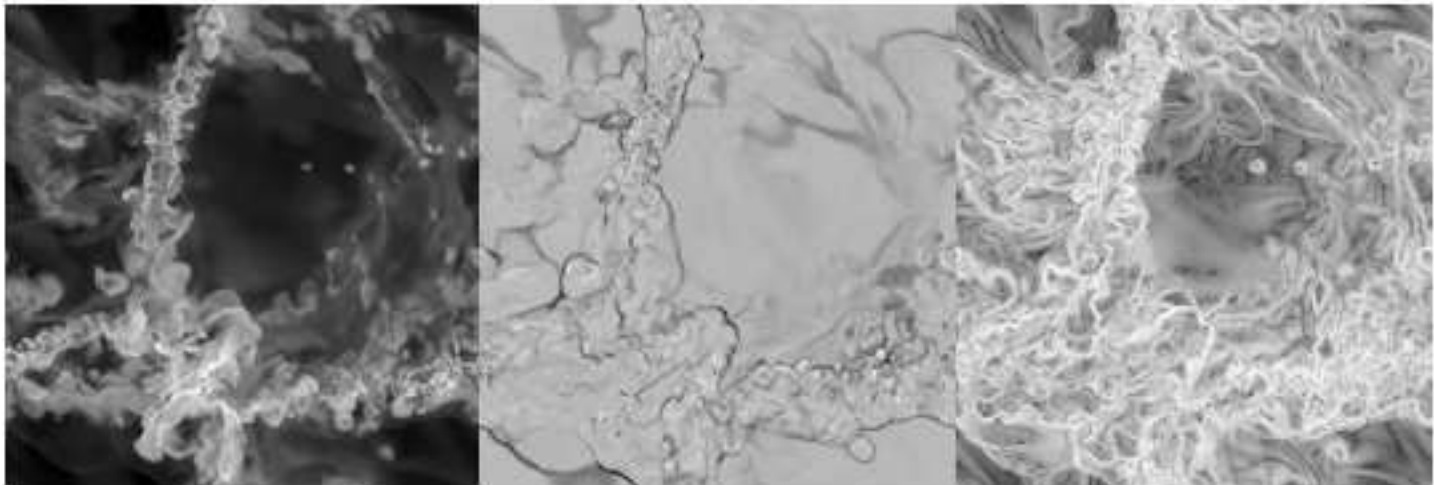


FIG. 1.— Snapshots of gas density ($\log \rho$, *left panel*), velocity divergence ($\nabla \cdot u$, *middle*), and vorticity magnitude ($(\nabla \times u)^2$, *right*), for a randomly chosen slice through the computational volume of 256^3 zones at $t = 0.12$ Myr. With a “standard” linear grey-scale color map dense structures in the left panel are shown as scrambled bright filaments, accretion shocks in the middle as sharp dark rims framing the cross-section of the density “walls”, and vortex filaments in the right panel as delicate freshly cooked Capelli d’Angelo covering the overdense regions and extending into underdense voids where the Kolmogorov cascade has not quite fully developed yet.

for ~ 0.05 Myr followed by a nonlinear regime characterized by formation of thermal pancakes – thin two-dimensional cool dense structures forming on caustics of the velocity field (Sasorov 1988). As the mean gas temperature drops and larger-scale modes enter nonlinear regime, small scale cellular network of thermal pancakes formed earlier in overdense regions collapses into larger-scale accretion shock-bounded cold dense structures. At the end of this *rapid cooling* stage gas temperature $T \in [30, 3 \times 10^5]$ K and the flow becomes highly supersonic with mass-weighted rms Mach number $\langle M \rangle_\rho$ in excess of 15. (A simulation initiated with flat “white noise” spectrum of density perturbations returned a substantially lower value $\langle M \rangle_\rho \lesssim 2$, highlighting the importance of large scale modes of TI for generation of supersonic flows.) Barotropic instabilities, shocks, and nonlinear thin shell instabilities (Vishniac 1994) coupled with TI effectively generate vorticity within the emerging cold dense phase. As a result, large scale thermal pancakes (Meerson & Sasorov 1987) arise turbulent.

Fig. 1 illustrates structures forming in the flow during early *turbulent relaxation* period. One can see shock-bounded “walls” and underdense “voids” in a slice through the computational box. The topology of dense structures in Fig. 1 is far richer than that of 2-D shock fronts in supersonic ideal gas turbulence. This snapshot taken at $t = 0.12$ Myr corresponds to the peak of volume-weighted rms Mach number, $\langle M \rangle_V \approx 3$. When cooling is present in nonequilibrium supersonic flows like this, thin high density shells get folded by instabilities into sheets of finite thickness with $D > 2$.

As turbulent relaxation proceeds, gas settles to thermal equilibrium and thermal phases get separated with about $\sim 18\%$ of the volume filled with the cold phase and $\sim 40\%$ with the warm phase by $t = 0.56$ Myr. As turbulence decays further, filling factors for both stable phases slightly grow at the expense of the intermediate thermally unstable regime. Since this two-phase medium is quasi-isobaric (with density variations well in excess of the pressure ones $\Delta p/p \approx 6 \ll \Delta \rho/\rho \approx 1000$) and velocities inherited from “violent relaxation” during the initial rapid cooling stage do not correlate with density, the Mach number depends on the gas density roughly as $M \propto \rho^{1/2}$, see Fig. 2. This means there are two different regimes of turbulence which

coexist in such a two-phase medium at $t = 0.56$ Myr: a subsonic regime with $M \sim 0.4$ in the space filling warm phase and a supersonic one $M \sim 1.5$ in the cold phase.

The Mach number–density relation is a distinct feature of turbulence in a two-phase medium. It is quite natural that velocity scaling relations in this case will not be identical to those for conventional compressible turbulence. It is also clear that reconstruction of these relations based on observations of any single phase in a multiphase medium would not be an easy task. We will further illustrate these ideas in the following section by formally applying statistical analysis methods developed for turbulence research to our simulation data.

3. VELOCITY STATISTICS

In order to follow the time evolution of the velocity field and the distribution of turbulent velocities across different scales, we computed three-dimensional velocity power spectra for four snapshots taken at $t = 0.12, 0.56, 1.5, 2.5$ Myr (Fig. 2). We also decomposed the velocity field into divergence-free *solenoidal* component u_s ($\nabla \cdot u_s = 0$, dotted lines) and curl-free *dilatational* component u_d ($\nabla \times u_d = 0$, dashed lines), such that $u = u_s + u_d$. As turbulence develops and decays the fractions of power contained in the solenoidal and dilatational components vary as a function of time and scale.

The first snapshot ($t = 0.12$ Myr) still keeps track of large-scale compressional forcing, the power spectrum is dominated by dilatational modes on large scales. A “wave” of solenoidal modes generated by the nonlinear instabilities propagates from small to large scales and overlaps with dilatational modes as turbulence develops. Earlier, at $t = 0.07$ Myr, the dilatational spectrum follows a nearly perfect k^{-2} law for the whole range of wavenumbers, characteristic of Burgers turbulence accompanying the formation of multiscale network of thermal pancakes. At that moment the contribution of solenoidal modes is negligibly small.

By $t = 0.56$ Myr, solenoidal modes dominate on virtually all scales. Dilatational modes decay much faster than solenoidal in an unforced regime that follows the initial phase transition. By $t = 1.5$ Myr they contribute only up to a few percent, thus the dotted and solid lines in Fig. 2 are nearly indistinguish-

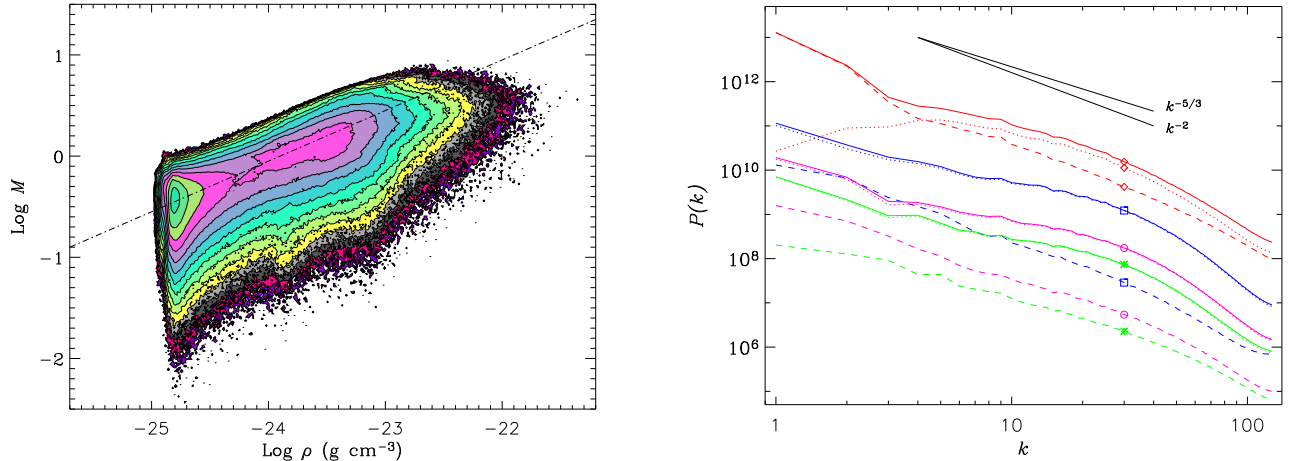


FIG. 2.— *Left panel*: Scatter plot of Mach number vs. gas density at $t = 0.56$ Myr; contour levels are consecutive powers of two, *dash-dotted line* follows the relation $M \propto \rho^{1/2}$ for isobaric gas with uncorrelated density and velocity. *Right panel*: 3-D Velocity power spectra (solid lines) for $t = 0.12$ (diamond), 0.56 (box), 1.5 (circle), and 2.5 Myr (asterisk) decomposed into solenoidal ($\nabla \cdot u_s = 0$, dashed lines) and dilatational ($\nabla \times u_d = 0$, dotted lines) components. Also shown are the characteristic velocity power spectrum scalings for Kolmogorov ($-5/3$) and Burgers (-2) turbulence.

able. The dependence of power in solenoidal vs. dilatational modes on the rms Mach number of the flow in our simulations is broadly consistent with results of Boldyrev, Nordlund, & Padoan (2002b) for driven isothermal MHD turbulence.

To study scaling properties of the decaying turbulent cascade we compute velocity structure functions (SFs) (Monin & Yaglom 1971)

$$S_p(l) = \langle |u(x) - u(x+l)|^p \rangle \propto l^{\zeta_p} \quad (1)$$

and exploit extended self-similarity (Benzi, et al. 1993, 1996) to obtain estimates for scaling exponents ζ_p relative to the third order exponent: $S_p \propto S_3^{\zeta_p/\zeta_3}$. These *relative* scaling exponents may be more universal than ζ_p themselves, since it is more natural to use a generalized scale $\ell(l, \eta)$ instead of the resolution scale l for investigation of scaling properties of turbulence (Dubrulle 1994). A value of ζ_3 is still required to recover the absolute values of the exponents ζ_p , e.g., to get an estimate for velocity power spectrum scaling in the inertial range $P(k) \propto k^{-1-\zeta_2}$. A rigorous result $\zeta_3 = 1$ holds for incompressible Navier-Stokes turbulence (Kolmogorov (1941b) “4/5” law) and for incompressible MHD (Politano, & Pouquet 1998). Numerical simulations support the same result for supersonic compressible hydrodynamics (Porter, Pouquet, & Woodward 2002, PPW02), but it is unclear whether this remains true in the presence of a generic volumetric energy source.

A three-parameter model developed by She & Lévéque (1994) and generalized by Dubrulle (1994) represents turbulent energy cascade as an infinitely divisible log-Poisson process and relates the dimensionality of the most dissipative structures D to the relative scaling exponents:

$$\frac{\zeta_p}{\zeta_3} = (1 - \Delta)\Theta p + \frac{\Delta}{1 - \beta}(1 - \beta^{\Theta p}), \quad (2)$$

where $\beta = 1 - \Delta/(3 - D)$ measures the “degree of nonintermittency” of energy dissipation, $\beta \in (0, 1)$. The other two parameters represent nonintermittent scalings for velocity difference: $u_l \propto l^\Theta$, and for eddy turnover time scale: $t_l \propto l^\Delta$. For the Kolmogorov cascade $\Theta = 1/3$ and $\Delta = 2/3$. In the limit $\beta \rightarrow 1$ the system is nonintermittent and K41 relation can readily be recovered. Since $\beta \rightarrow 0$ as $D \rightarrow 2\frac{1}{3}$, the model is only consistent with $D < 2\frac{1}{3}$. Vortex filaments in incompressible turbulence are characterized by $D = 1$ with which eq. (2) reduces to SL94

formula. In a series of numerical experiments on isothermal compressible turbulence with Mach numbers $0.62 \leq M \leq 10$, Padoan et al. (2003) were able to trace a smooth transition from scalings which can be approximated by eq. (2) with $D = 1$ to those with $D = 2$. Their result is consistent with the suggestion that velocity SF scaling for compressible turbulence can be described by the She-Lévéque formalism for any value of the Mach number of the flow, with only one parameter, D , varying as a function of M .

What kind of scaling can we expect for our model with “realistic” non-isothermal scale-dependent effective equation of state determined by cooling and heating? How will it evolve as turbulence decays and the two phases settle into thermal and pressure equilibrium?

We computed velocity SFs up to the 6th order using the so-called “XYZ method” (see, e.g., PPW02). Relative scaling exponents for the same four snapshots that we used for power spectra are shown in Fig. 3. The insert shows generation and decay of kinetic energy within the box, positions of the four snapshots on the decaying branch are indicated by different symbols, respectively. We consider the difference between exponents for longitudinal and transverse SFs as a good quality indicator for the derived scalings (larger symbols show larger statistical uncertainties). We attribute differences between longitudinal and transverse SFs to poor statistics and to small deviations from full isotropy in our numerical model due to insufficiently large value of Reynolds number and slightly anisotropic initial forcing on scales approaching the box size.

Our results generally agree with those of Padoan et al. (2003) in the sense that the exponents in Fig. 3 can be well described by eq. (2) and, as the turbulence decays and becomes less supersonic, $D \rightarrow 1$. However, for a given turbulent Mach number the value of D appears to be larger in our multiphase case than in the isothermal turbulence. This could potentially be caused by the possibility that $\zeta_3 < 1$ in our case; higher resolution simulations would help to test this option. It is tempting to note that our first snapshot (diamonds), which corresponds to the most supersonic regime with no clear distinction between the thermal phases, demonstrated the maximal value of D for this run which is approaching the upper bound of $2\frac{1}{3}$. Curiously enough, this value coincides with observationally determined fractal dimension of molecular clouds $D = 2.3 \pm 0.3$ (Elmegreen & Falgarone

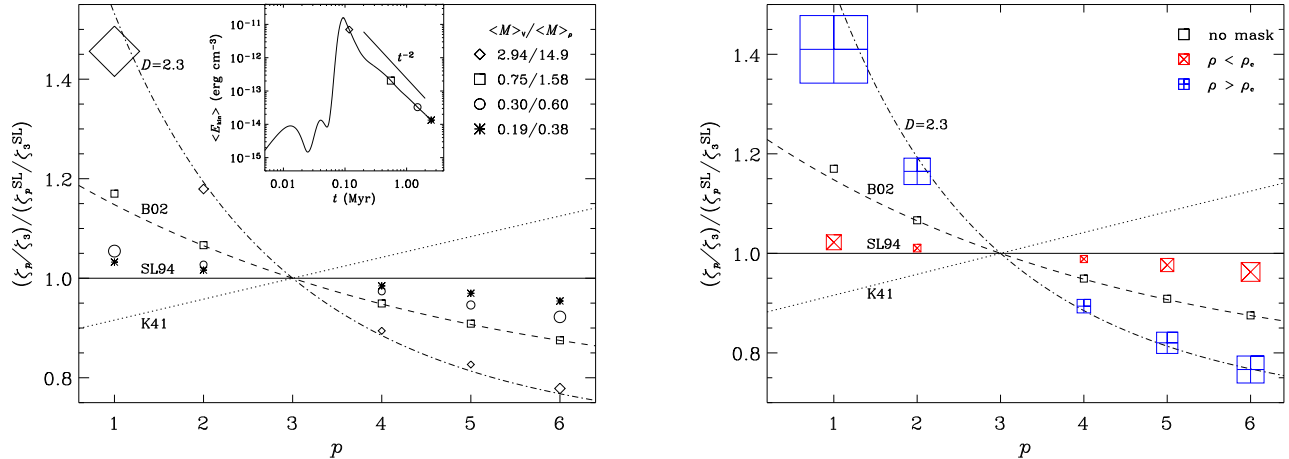


FIG. 3.— Scaling exponents for velocity structure functions of the orders 1 to 6 normalized by SL94 model (*horizontal solid line*); other models include: K41 (*dotted line*), B02 (*dashed line*), and eq. (2) with fractal dimension $D = 2.3$ (*dash-dotted line*). Symbol sizes show the difference between the longitudinal and transverse structure functions with a floor value. *Left panel*: Four snapshots illustrate the evolution of the scaling. Insert shows the kinetic energy as a function of time and timing for the snapshots: 0.12 Myr – *diamonds*, 0.56 Myr – *boxes*, 1.5 Myr – *circles*, 2.5 Myr – *asterisks*. Legend in the upper right corner gives volume- and mass-weighted rms Mach numbers for the snapshots. *Right panel*: Scaling exponents for a snapshot at $t = 0.56$ Myr. *Open boxes* are the same as in the left panel; *crossed boxes* show the exponents obtained with density masks $\rho \gtrsim \rho_c = 10^{-24.3}$ g cm $^{-3}$ and probe velocity correlations in the cold and warm phases separately.

1996). We refer to Boldyrev et al. (2002b) for a relation between density and velocity correlators. It seems, however, that it is not the limited numerical resolution, but rather the lack of cooling-related instabilities, that prevents dense structures to fold into a fractal distribution with dimensionality $D \gtrsim 2$ in simulations of isothermal turbulence, cf. (Boldyrev, Nordlund, & Padoan 2002a).

Observational diagnostics of turbulent velocity fluctuations in interstellar medium are usually based on phase-specific spectral line transitions. Since we model the formation of a turbulent two-phase medium, it is natural to compute SFs by measuring the velocity differences within a single phase and then compare results for both phases. We introduced two masks based on a gas density value $\rho_c = 10^{-24.3}$ g cm $^{-3}$ and obtained velocity SFs separately for zones where the gas density is higher or lower than the threshold ρ_c , which close to the lower bound of thermally unstable regime (for gas in thermal equilibrium) and, thus, separates the warm stable phase from cold “clouds” and unstable gas. At $t = 0.56$ Myr, the filling factors for both density regimes are about 50%. The warm gas is mostly subsonic and evolves in a quasi-isothermal regime, while the cool gas is still essentially supersonic, see Fig. 2.

The scaling exponents for velocity SFs of low- and high-density gas are shown in Fig. 3. The statistics for both density regimes are relatively poor as is indicated by the size of the crossed symbols. They are good enough, however, to conclude that the cold phase exponents show significantly larger departures from K41 scalings than do the complete statistics unaf-

fected by masking. Crossed symbols representing the warm phase instead demonstrate more K41-like scalings. Both transverse and longitudinal SFs follow the trend outlined above, but the exponents for transverse SFs show consistently smaller departures from the unbiased exponents. We conclude that velocity power spectrum index n_c based on observations of the cold molecular phase would be rather an upper estimate for the actual index $n = 1 + \zeta_2$, while n_w determined from the warm gas velocities would only give a lower bound for n .

4. CONCLUSIONS

We considered a simple model for TI-induced decaying hydrodynamic turbulence in a radiatively cooling medium with a low constant heating rate. A formal application of She & Lévéque (1994) model to the simulated velocity fields consistently showed that cooling-related instabilities make turbulence in multiphase gas more intermittent than conventional compressible supersonic turbulence. This result could have interesting implications for recently developed turbulent fragmentation branch of star formation theory. Finally, we demonstrated that phase-specific observational velocity statistics for multiphase media can be affected by the correlation of turbulent Mach number with gas density.

We acknowledge useful discussions with Paolo Padoan. This work was partially supported by NRAC allocation MCA098020 and utilized computing resources provided by the San Diego Supercomputer Center.

REFERENCES

- Armstrong, J. W., Rickett, B. J., & Spangler, S. R. 1995, *ApJ*, 443, 209
 Benzi, R., Ciliberto, S., Tripiccone, R., Baudet, C., Massaioli, F., Succi, S. 1993, *Phys. Rev. E*, 48, R29
 Benzi, R., Biferale, L., Ciliberto, S., Struglia, M.V., Tripiccone, R. 1996, *Physica D*, 96, 162
 Blondin, J. M. & Marks, B. S. 1996, *New Astronomy*, 1, 235
 Boldyrev, S. 2002, *ApJ*, 569, 841 (B02)
 Boldyrev, S., Nordlund, Å., & Padoan, P. 2002a, *ApJ*, 573, 678
 Boldyrev, S., Nordlund, Å., & Padoan, P. 2002b, *Phys. Rev. Lett.*, 89, 31102
 Brunt, C. M. & Heyer, M. H. 2002, *ApJ*, 566, 289
 Colella, P. & Woodward, P. R. 1984, *J. Comp. Phys.*, 54, 174
 Dubrulle, B. 1994, *Phys. Rev. Lett.*, 73, 959
 Elmegreen, B. G. & Falgarone, E. 1996, *ApJ*, 471, 816
 Field, G. B. 1965, *ApJ*, 142, 531
 Field, G. B., Goldsmith, D. W., & Habing, H. J. 1969, *ApJ*, 155, L149
 Kolmogorov, A. N. 1941a, *DAN SSSR*, 30, 299 (K41)
 Kolmogorov, A. N. 1941b, *DAN SSSR*, 32, 19
 Kritsuk, A. G., & Norman, M. L. 2002, *ApJ*, 569, L127
 Kritsuk, A. G., & Norman, M. L. 2002, *ApJ*, 580, L51
 Larson, R. B. 1979, *MNRAS*, 186, 479
 Larson, R. B. 1981, *MNRAS*, 194, 809
 Meerson, V. I., & Sasorov, P.V. 1987, *Sov. Phys. JETP*, 65, 300

- Monin, A. S., & Yaglom, A. M. 1971-75, Vol. 1-2, Statistical Fluid Mechanics; Mechanics of Turbulence (Cambridge, MA: MIT Press)
- Vishniac, E. T. 1994, ApJ, 428, 186
- Padoan, P. & Nordlund, Å. 2002, ApJ, 576, 870
- Padoan, P., Jimenez, R., Nordlund, A., & Boldyrev, S. 2003, astro-ph/0301026
- Pikel'ner, S. B. 1968, Sov. Astron., 11, 737
- Politano, H., Pouquet, A. 1998, Geophys. Res. Lett., 25, 273
- Porter, D., Pouquet, A., & Woodward, P. 2002, Phys. Rev. E, 66, 026301 (PPW02)
- Sasorov, P. V. 1988, Sov. Astron. Lett., 14, 129
- She, Z.-S., & Lévêque, E. 1994, Phys. Rev. Lett., 72, 336 (SL94)